# Areal Surface Characterization of Acid Fractures in Carbonate Rocks

Valdo F. Rodrigues, Ana C. R. Medeiros, Northern Fluminense University, Rodolfo A.Victor, Petrobras/RH/UP, Wellington Campos, Petrobras/E&P



This paper was prepared for presentation during the 12th International Congress of the Brazilian Geophysical Society held in Rio de Janeiro, Brazil, August 15-18, 2011.



## Abstract

Fracture surface characteristics have significant effect on fracture hydraulic conductivity. The available acid-fracture conductivity correlations do not consider surface characteristics or make an incipient use of it. A proper description of the acid-fracture surfaces is the initial step towards the right consideration of surface roughness in hydraulic conductivity. This paper presents an areal (3D) surface evaluation of acid-etched fractures, simulated in samples taken from whole cores of an oil producer limestone. The topography of acid-fractured surfaces was assessed using a laser profilometer. The surfaces were evaluated with a set of 3D surface parameters. The results showed that the main features of acid-etched surfaces are large roughness, negative skewness, high kurtosis, and intermediate isotropy, mostly random but with some spatial orientation. The acid-fractured surfaces can be represented by the rms height, which showed great linear correlation with most of the surface parameters. The parameters texture aspect ratio, bearing index, valley retention index, and density of summits showed low correlation with rms height. A method to calculate fracture width from surface topography was developed. An attempt to explain abnormal behavior in initial conductivity tests revealed the potential use of surface characterization for fines management in oil and gas reservoirs. Improved acid fracture correlation may be achieved using surface characterization parameters.

## Introduction

Acid fracturing is a well stimulation method used in oil and gas reservoirs of acid soluble rocks. To create an acid fracture acid is pumped along a hydraulically induced fracture, leaking off into the formation. After pumping stop, hydraulic pressure falls, the higher fracture faces asperities contact each other and deform under closure stress (**Fig. 1**). The most important parameters for acid fracturing success are fracture conductivity and fracture length. The current acid fracture conductivity correlations present low accuracy, so there is a demand for improved correlations.

Acid fracture conductivity depends on fracture width, fracture surface roughness, and fracture faces mismatch. Surface characterization is essential to estimate the roughness effects and can be used to calculate the mechanical width, providing results more accurate than usual lab measurements.

Profile surface characterization has been applied in fracture conductivity studies (Patir and Cheng, 1978; Brown and Scholz 1985; Zimmerman and Bodvarsson, 1994; Gong *et al.*, 1998). Recent studies applied areal surface characterization in acid fractures with 3D visualization techniques and calculating some 3D parameters (Malagon, 2008; Pournik, 2008; Antelo *et al*. 2009). This work differentiates from previous studies by using samples from whole cores of an oil producer limestone, instead of samples from quarries or outcrops, and by evaluating the fracture surfaces with a comprehensive areal surface characterization. A method to calculate fracture width from surface topography was developed. A trial to explain abnormal behavior in initial conductivity tests revealed the potential use of surface characterization for fines management in oil and gas reservoirs.

## Experimental study procedures

Five meters of whole cores from the Quissamã limestone, Campos Basin, offshore Brazil, taken from 3,515.5 m to 3,545.5 m depth, were cut and polished to the shape of the modified API cell used for acid fracture simulation and conductivity tests **(Fig. 2)**. The cores provided 20 samples of 17.78 cm (7 in.) length, 4.44 cm (1.75 in.) height, and 7.62 cm (3 in.) thickness. Then the following sequence of tests was carried out:

1. Profilometer scan of each sample before acid-etching;
2. Acid-etching along the fracture mimic by each pair of samples;
3. Profilometer scan of each sample after acid-etching.

The injection rate during acid etching was set at 1.0 L/min in all experiments, with a backpressure of 6.89 GPa (1,000 psi). Four acid systems were used: straight 15% HCl, gelled 15% HCl, viscoelastic 15% HCl, and emulsified HCl at 185°F. The acid-etching was properly scaled to field conditions based on Reynolds' and on Peclet's dimensionless numbers.

The laser profilometer used to assess surface topography (**Fig. 3**) had vertical accuracy of 13 µm (0.0005 in.) and measurement range of 25.4 mm (1.0 in.). All the experiments used a 0.05 inch measurement interval in both directions. The profilometer recorded the scanning data in three columns, two for position and the third for

the height, so that each row corresponded to 3D coordinate.

**Parameters selection for areal characterization of acid fracture surfaces**

The transition from profile to areal characterization has been considered part of the current paradigm shift in surface metrology. The areal characterization tries to identify the fundamental and functional topographical features of the surface. It includes evaluation of texture shape and direction and discrimination between connected and isolated features (Jiang et al 2007).

This study adopted a suit of parameters mostly from the ones proposed in the ISO/TS CD 25178-2 (2006) standard. The parameters selection followed two criteria: address the hydraulic conductivity function and present reliable method of calculus. The selected suit included the amplitude parameters rms height (Sq), height skewness (Ssk), height kurtosis (Sku), maximum peak height (Sp), maximum valley height (Sv), maximum height of texture surface (Sz), and arithmetical mean height (Sa). It also included the spatial parameters: fastest decay auto-correlation length (Sal), texture aspect ratio (Str), and texture direction of the texture surface (Std). Idem the hybrid parameters rms slope of the assessed texture surface (Sdq) and developed interfacial area ratio (Sdr). From the 13 parameters of the so called volume set four were selected: material volume of peaks (Vmp), material volume of the core (Vmc), void volume of the core (Vvc) and void volume of the valleys (Vvv). Three parameters, not included in the standard, were added: surface bearing index (Sbi) , core fluid retention index (Sci), valley fluid retention index (Svi). From the nine feature parameters four were selected: density of summits (Sds), ten-point height of surface (S10z), five-point peak height (S5p), and five-point pit height (S5v).

The areal surface texture parameters were calculated on the roughness area after filtering out form and waviness. The filter used is the one recommended in the ISO-13565-1 (1998) standard, proper for surfaces with deep valleys such as the acid wormholes. It was implemented with a moving average algorithm. To calculate the parameters this study implemented the equations presented by Dong, *et al.* (1993), Thomas (1999), Mainsah, *et al.* (2001), Whitehouse (2002), and Blunt and Jiang (2003) with MATLAB codes. The parameters Sal, and Str were obtained with a specific code that first calculated the normalized autocorrelation function, and then the contour line related to the 0.2 decay, and finally calculated its minimum and maximum intercept segments. The minimum segment corresponds to Sal and the minimum to maximum segment ratio corresponds to Str (Tsukada e Sasajima 1983, *apud* Thomas 1999).

**Definition of the area of analysis**

Some artifacts from the apparatus and procedures used in the experimental study were reported in previous tests (Pournik 2008). Thus this study carried out a sensitivity analysis to define the area of surface evaluation. This was done by gradually excluding rows and columns of data matrix and checking the stability of parameters values. **Fig. 4** illustrates the process and its results. The exclusion of obvious outliers close to the sample borders formed the general area of analyses. This required an exclusion of 2.54 cm (1.0 in.) at both ends along the length (X). Regarding the height (Y) it was necessary to reject 1.25 cm (0.50 in.) in both laterals. Focusing the area of analysis for conductivity purposes the choice was to adopt the region of back conductivity (Fig. 4). This is the most representative area for conductivity tests because almost all the pressure loss that allows conductivity calculation occurs in this area.

**Core preparation evaluation**

The fractures were not hydraulically created in the laboratory, but simulated with flow inserts between each pair of samples. The initial surface analysis of the samples before acid etching showed some abnormal valleys on the sample borders, which had to be removed for surface analysis before acid-etching by means of excluding a 1.14 cm strip along the borders. The analysis then showed Sa range from 15 µm to 106 µm, Ssk range from -18.8 to -3.9, and Sku range from 22.2 to 502.8. It seems that large range of heights and negative skewness are features of the studied carbonate, while the high kurtosis derived from sample preparation imperfections. A comparison of the fractures surfaces mimic in this study with surfaces of fractures obtained by tension (Brazilian test) would be useful to verify possible influences of the lab process on the acid-etched surfaces.

**Areal surface analysis of the acid-etched surfaces**

The acid etched surfaces evaluation was based on 3D visualization techniques and descriptive statistics. The aim of the visualization techniques is to enable the human eyes to visualize features that are hard to see without the aid of these techniques. This can be achieved by use of colors, different views, and scale magnification. **Fig. 5** shows an unfiltered color 3D surface graph, which illustrates hydrodynamic effects on the samples entrance. **Fig. 6** shows a Z inverted gray 3D surface graph of sample 4B, which emphasizes the valleys. **Fig. 7** shows the roughness of sample 5A. **Fig. 8 and 9** show the areal autocorrelation function and respective contour line for the sample 5A (Str = 0.76), while **Fig. 9 and 10** show the same for the sample 1A (Str = 0.31). One can see some spatial orientation even in the more random sample (Fig. 8 and 9).

Starting the numerical analysis with the measures of central tendency and shape Sa range was 44 µm to 597 µm with an average of 207 µm, and 146 µm standard deviation (SD). This range is far above the typical roughness values of engineering surfaces obtainable by different finishing processes (Whitehouse, 2002), which Ra values (the 2D equivalent of Sa) vary from 0.05 µm to 25 µm. Sq range was 72 µm to 1253 µm, with an average of 349 µm, and 279 µm SD. Ssk varied from –2.8 to -4.4, with -2.8 mean, while Sku range was 6.1 to 30.8 with 13.7 mean. Thus, large roughness, negative skewness, and high kurtosis are features of the evaluated acid-etched fractures.

The high values of the peak and valleys parameters confirm that acid-etched surfaces are very rough. Comparing with some engineering surfaces (Blunt e Jiang 2003) they present height ranges 39 times or more larger than those **(Table 1)**. This reflects on other parameters.

The autocorrelation function (AACF) is a useful tool for acquiring information about the spatial properties of surfaces (Mainsah *et al*., 2001). It provided the parameters Sal and Str, as well as the figures of AACF and contour line (relative to the normalized AACF drops to 0.2). The smallest lag length at which the AACF decays to 0.2, Sal, varied from 1.5 mm to 24.7 mm with 6.2 mm mean and 7.2 mm SD. Great values of Sal denote the predominance of low frequency components. The texture aspect ratio, Str, range was 0.31 to 0.84 with 0.60 mean and 0.14 SD. Str varies from 0.00 (fully anisotropic surfaces) to 1.00 (fully isotropic surfaces). Any surface with Sdr > 0.50 would have significant multi-directional regularity, while those with Sdr < 0.3 would be strongly anisotropic (Mainsah *et al*., 2001). The Str values show that most of the studied acid fracture surfaces are predominantly isotropic. However, as backed by the AACF figures, some spatial orientation can be seen even in the more isotropic surfaces (Fig. 8).

The Std values were not considered because according to Mainsah *et al.* (2001) they are meaningless for surfaces predominantly isotropic (Str > 0.5).

The hybrid parameter Sdq range was 0.08 to 1.13 with 0.37 mean and 0.27 SD, while Sdr varied from 0.5% to 58.5% with 12.0% mean and 14.0% SD. Sdr is the preferred hybrid parameter because it is less affected by scale effects and method of calculus (Mainsah *et al.* 2001) and appears more tangible to flow along fractures. **Table 3** shows Sdr values for a grit blasted surface and a worn surface (Blunt and Jiang, 2003) and for samples 2B and 6B.

Sds range was 0.004 $mm^{-2}$ to 0.049 $mm^{-2}$ with 0.031 $mm^{-2}$ mean and 0.013 $mm^{-2}$ SD. Sds is related to the mode in which the summits deform under load. Low values of Sds may result in higher localized contact stresses ensuing the generation of fines (Michigan Metrology, 2011).

The parameters of the category volume showed high range of values. Those related to the upper part of the material rate curve, in particular Sbi, indicate the chance of fines generation while those related to the lower part of the curve indicate the surface capacity to storage fines and allow its flow (Michigan Metrology, 2011).

This study used the coefficient of linear correlation, r, to estimate the correlation between each pair of parameters. The range of r is -1.00 to 1.00. A value of zero indicates no linear relationship between two variables, whereas the closer the value is to 1 or -1, the greater the relationship, positive or negative, respectively, between the variables. This is valid only for descriptive purposes because the distributions obtained in this study are not Gaussian (Salkind, 2007). Taking Sq as a reference it showed great correlation (r > 0.70) with most of the parameters and low correlation with: Sci (r =-0.60), Sds (r = -0.55), Svi (r = 0.40), Sbi (r = -0.24) e Str (r = 0.05). Any of the parameters highly correlated with Sq could represent the acid fracture surfaces. However, Sq is preferred because it is less sensitive to skewed data and to outliers (Salkind, 2007), and also to anomalous bright spot on the sample (Malagon 2007). Besides, it has been used in previous 2D characterization studies (Patir e Cheng 1978; Walsh 1981; Zimmerman e Bodvarsson 1994). Note that Ssk and Sku are not good parameters for correlation because they can lead to misinterpretations when applied to non Gaussian distribution.

### Fracture width calculus

Fracture width is the main determinant of fracture conductivity at zero closure stress in acid-fracture conductivity correlations (Nierode and Kruk, 1973; Pournik, 2008). The usual laboratory estimative based on samples mass difference, before and after acid flow, is not accurate because of acid-rock reactions residues. The use of surface topography to calculate fracture width appears to provide more accurate values. The method developed in this study, initially figures out the maximum relative distance between two juxtaposed samples, then computes locally the difference between the maximum and the local height sum, and finally takes the average across the area. The mean of width on the area of analysis was denominated $w_{topm}$ (**Table 3**).

### Conductivity tests abnormalities analysis

In the initial conductivity tests three out of ten behaved far from the expected exponential decay. An attempt to explain these abnormalities with surface characteristics failed because the analysis showed that leaks were probably the main cause of problems and masked other possible causes. However there were evidences of possible fines generation and partial retention in a couple of tests associated with low values of Sbi, Sds, and Sq (and consequently, by correlation, low values of width and valleys parameters). While low values of Sbi and Sds indicate high chance of fines generation, low values of width and valleys parameters indicate low capacity to storage fines and allow their movement. Although not conclusive, this qualitative analysis revealed the potential of surface characterization use in fines management, an important issue in oil and gas reservoirs.

### Conclusions

The core samples surfaces before acid-etching showed large range of heights, negative skewness, and very high kurtosis.

The studied acid-etched fracture surfaces showed roughness much larger than usual engineering surfaces, negative skewness, high kurtosis, and an intermediate isotropy - mostly random but with some spatial orientation.

The acid-fractured surfaces can be represented by the rms height, which showed high linear correlation with most of the surface parameters, complemented with the parameters that showed low correlation: texture aspect

ratio, bearing index, valley retention index, and density of summits.

An attempt to explain abnormal behavior in the initial conductivity tests illustrated the potential use of surface characterization in fines management in oil and gas reservoirs.

Three themes for further studies are suggested. The first is to search new acid fracture conductivity by checking the fitness between surface parameters and measured conductivities. The second is to evaluate the use of surface characterization in fines management in oil and gas reservoirs. The third is to evaluate the surfaces of fractures produced by longitudinal tension (Lobo Carneiro or Brazilian Test) and compare the results with the ones generated in this study.

### Acknowledgments

The authors gratefully acknowledge the National Agency of Petroleum, Natural Gas, and Bio-combustible, ANP, for allowing the use of cores of Quissamã limestone. Special thanks go to Osvaldo de Oliveira Duarte for his invaluable suggestions

### References

Antelo, L.F., Pournik, M., Zhu, D., and Hill, A.D. 2009. Surface Etching Pattern and its Effect on Fracture Conductivity in Acid Fracturing. Paper SPE 119743 presented at the Hydraulic Fracturing Technology Conference, Woodlands, Texas, USA, 19-21 January.

Blunt, L. e Jiang, X. 2003. Advanced techniques for assessment surface topography – development of a basis for 3D surface texture standards SURFSTAND, Kogan Page Science, Elsevier Ltd.

Brown, S.R. and Scholz, C.H. 1985. Broad bandwidth study of the topography of natural rock surfaces. *J. Geophys. Res.9***0**(B14):12575-12582.

Dong, W. P., Mainsah, E., Stout, K. J. and Sullivan, P. J. 1994. Three Dimensional Surface Topography - A review of Present and Future Trends, In K. J. Stout (ed), Three-Dimensional Surface Topography-Measurement, Interpretation and Applications, Penton Press,London.

Gong, M., Lacote, S., and Hill, A.D. 1999. A New Model of Acid Fracture Conductivity Based on Deformation of Surface Asperities. Paper SPE 39431 presented at the International Symposium on Formation Damage Controle, Lafayette, Lousiana, USA, 18-19 February.

ISO-13565-1 1998 *Geometrical Product Specifications (GPS) - Surface texture: Profile method; Surfaces having stratified functional properties - Part 1: Filtering and general measurement conditions*.

ISO/TS CD 25178-2: 2006 *Geometrical product specification (GPS)—surface texture: areal—part 2: terms, definitions and surface texture parameters*.

Jiang, X, Scott, P.J., Whitehouse. D. J. e Blunt, L: "Paradigm shifts in surface metrology. Part II. The current shift" *Proc. R. Soc. A* 2007 **463**, 2071-2099, *Proc. R. Soc. A* 2007 **463**, 2071-2099

Mainsah, E., Greenwood, J.A., and Chetwynd, D.G.: "Metrology and Properties of Engineering Surfaces", Kluwer Academic Publishers, Boston, 2001. ISBN 0-412-80640-1

Malagon Nieto, C. 2007. 3D Characterization of Acidized Fracture Surfaces. MsC dissertation, Texas A&M University, May 2007.

Michigan Metrology, http://www.michmet.com/3d, accessed 25 January 2011.

Nierode, D.E. and Kruk, K.F. 1973. An Evaluation of Acid Fluid Loss Additives, Retarded Acids, and Acidized Fracture Conductivity. Paper SPE 4549-MS presented at the 1973 SPE Annual Fall Meeting, Las Vegas, Nevada, USA, 30 September-3 October.

Patir, N. and Cheng, H.S. 1978. An average flow model for determining effects of three-dimensional roughness on partial hydrodynamics lubrication. J. Lubr. Technol. 100, 12-17.

Pournik, M. 2008. Laboratory-Scale Fracture Conductivity Created by Acid Etching. PhD dissertation, Texas A&M University, College Station, Texas, USA.

Salkind, N.J., Editor: Encyclopedia of Measurement and Statistics, Vol , SAGE Publications, Inc., Thousand Oaks, California, 2007

Stout, K. J., Sullivan, P. J., Dong, W. P., Mainsah, E., Luo, N., Mathia, T., Zahouani, H. (1993) *The development of methods for the characterization of roughness **in** three dimensions,* Commission of the European Communities, EUR 15178 EN, Brussels - ISBN *0*-7044-1313-2.

Thomas, T. R. 1999. Rough Surfaces, Second edition. Imperial College Press.

Whitehouse, D. 2002. Surfaces and their Measurement. Kogan Page Science Paper Edition.

Zimmerman, R.W., and Bodvarsson, G.S. 1994. Hydraulic Conductiviy of Rock Fractures, Earth Sciences Division Lawrence Berkeley Laboratory University of California Berkeley, CA 94720, October 1994

Zou, C. 2006. Development and Testing of and Advanced Acid Fracture Conductivity Apparatus. MsC dissertation, Texas A&M University, College Station, Texas, USA.

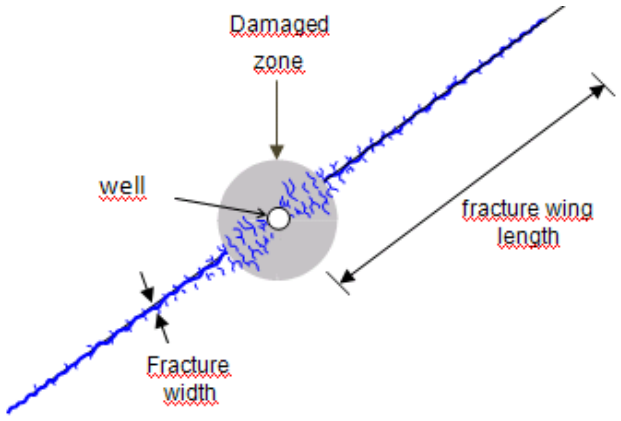


**Fig. 1**-*Schematics of a well stimulated with an acid fracture. * Out of scale: fracture width highly magnified.*

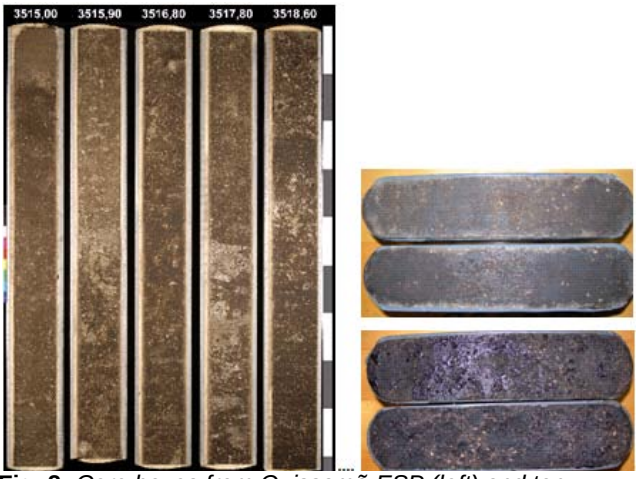


**Fig. 2**- *Core boxes from Quissamã-ESP (left) and top view of samples before (above) and after (below) acid etching.*

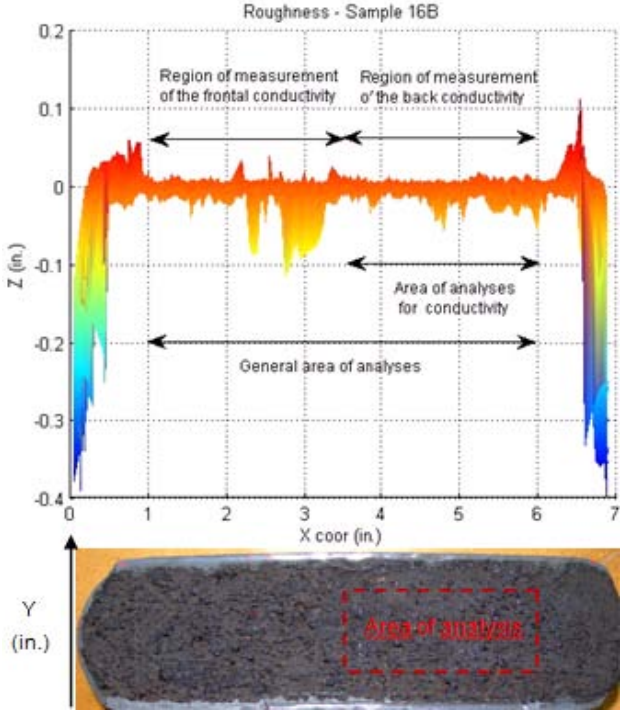


**Fig. 4-***Illustration of the areas of analyses*
** Z scale amplified 10 times*

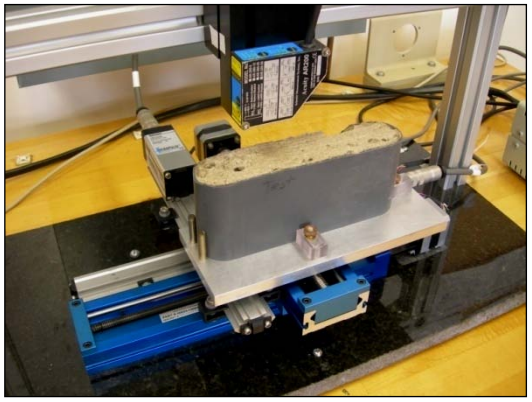

**Fig. 3-***Profilometer scanning after acid etching*
** Note wormholes on acid-etched face***.**

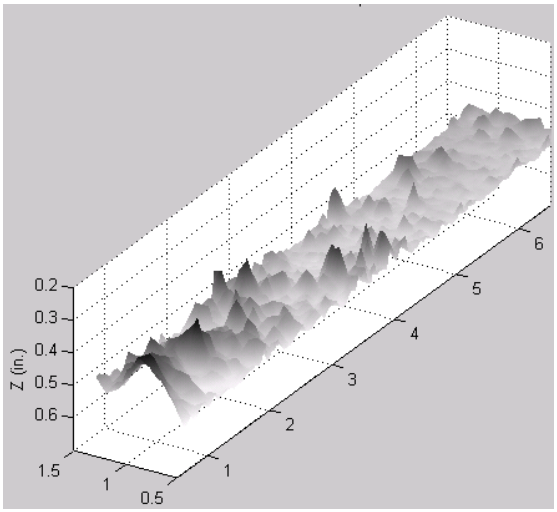


**Fig. 5-***Unfiltered Z inverted 3D graph – sample 4B*
** Z scale amplified 3 times.*

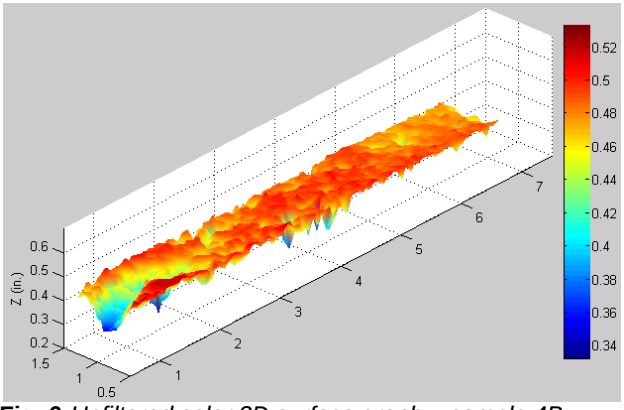


**Fig. 6-***Unfiltered color 3D surface graph – sample 4B*
** Z scale amplified 3 times.*
** Note high localized dissolution at the entrance.*

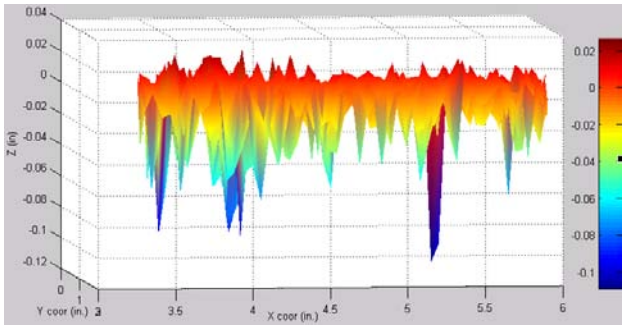


**Fig.7-***Roughness– sample 5A. * Z scale amplified 10 times. * Note the deep valleys (wormholes).*

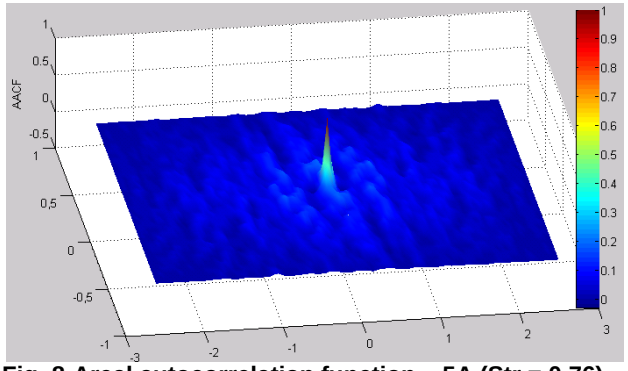


**Fig. 8-Areal autocorrelation function – 5A (Str = 0.76)**

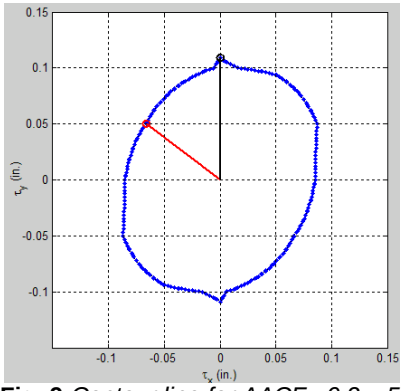


**Fig. 9-***Contour line for AACF= 0.2 – 5A*

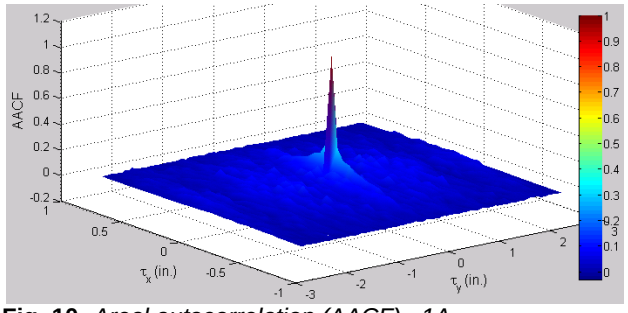


**Fig. 10-** *Areal autocorrelation (AACF) –1A (Str = 0.31)*

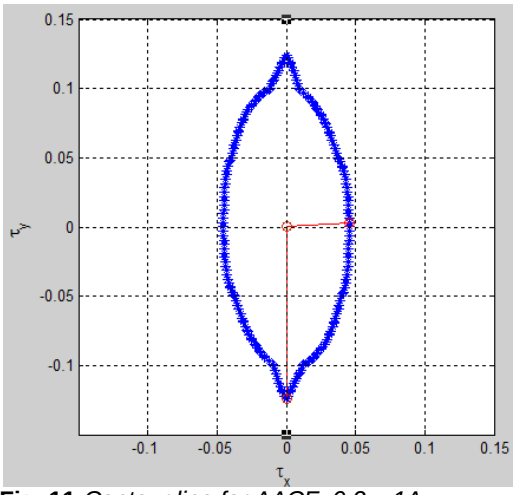


**Fig. 11-***Contour line for AACF=0.2 – 1A*

**TABLE 1-** *AMPLITUDE PARAMETERS COMPARISON*

| Parameter/ Surface | Honed surface | Ground surface | Sample 14 |
|---|---|---|---|
| Sampling area (mm x mm) | 3 x 3 | 2 x 2 | 63.5 x 25.4 |
| Height range (µm) | 0.00 to 14.37 | 0.00 to 3.22 | -476 to 82 |
| Sq (µm) | 1.23 | 0.423 | 82 |
| Ssk | -3.148 | 0.101 | -2.67 |
| Sku | 13.219 | 3.113 | 9.40 |
| Sp (µm) | 0.552 | 1.536 | 83.06 |
| Sv (µm) | -13.819 | -1.682 | -476 |
| Sz (µm) | 14.371 | 3.218 | 560 |
| | Blunt and Jiang 2003 | | |

**TABLE 2-***Sdr VALUES FOR FOUR SURFACES*

| Parameter/ Surface | Grit blasted surface | Worn surface | Sample 2B | Sample 6B |
|---|---|---|---|---|
| Sampling area (mm x mm) | 9.07 x 12.14 | 9.07 x 12.14 | 63.5 x 25.4 | 63.5 x 25.4 |
| Height range (µm) | 0.00 to 17.55 | 0.00 to 15.20 | -1015.74 to 217.68 | -1130 to 82 |
| Sdr | 5.51 % | 3.04 % | 0.81% * | * 58.50% |
| | Blunt and Jiang 2003 | | | |

* Minimum and maximum values of Sdr

**TABLE 3-***FRACTURE WIDTH ($w_{topm}$)*

| Sample | 1&2 | 3&4 | 5&6 | 7&8 | 9&10 |
|---|---|---|---|---|---|
| Width (mm) | 0.413 | 1.08 | 1.74 | 1.32 | 1.60 |
| Sample | 11&12 | 13&14 | 15&16 | 17&18 | 19&20 |
| Width (mm) | 1.41 | 0.62 | 1.29 | 0.566 | 0.945 |